The effect of the electron-electron interaction on the Lifshitz transition density in bilayer graphene

Csaba Tőke and Vladimir I. Fal'ko
Department of Physics, Lancaster University, Lancaster, LA1 4YB, United Kingdom
(Dated: March 13, 2009)

We study the renormalization of the effective mass and trigonal warping of bilayer graphene by the electron-electron interaction. One consequence of such a renormalization in the low-energy bands of a bilayer crystal consists of a small reduction of the critical density of the Lifshitz transition (the crossover between the single-pocket and four-pocket topology of the Fermi surface).

PACS numbers: 71.10.Ca, 71.18.+y, 71.70.Gm

The bilayer graphene crystal is one of several allotropic forms of carbon one can fabricate using micro-mechanical cleavage of bulk graphite[1]. The crystalline structure of bilayer graphene is derived from the Bernal stacking[2] of layers in the "mother" graphite crystal. It is shown in Fig. 1(a) as two hexagonal carbon lattices with inequivalent sites A, B (bottom layer) and $\widetilde{A}, \widetilde{B}$ (top layer) such that the $\widetilde{A}$ sites are above the B sites, while A ($\widetilde{B}$) is located above (below) the midpoint of a hexagon on the other layer. Theoretical studies[3], transport[1], ARPES[4] and optical[5] characterization of bilayer graphene have indicated that this material is a gapless semiconductor with two split-bands separated by $\pm\gamma_1$, where γ_1 is the closest-neighbor interlayer ($\widetilde{A}B$) coupling, and two "low-energy" almost parabolic bands with effective mass determined by both γ_1 and the intralayer coupling γ_0.

Detailed tight-binding model studies[3] of bilayer graphene taking into account the next-neighbor ($\widetilde{B}A$) interlayer coupling γ_3 have indicated that the dispersion of the low-energy bands in it is strongly anisotropic at small momenta $p \sim \gamma_3\gamma_1/(\gamma_0^2 a)$, with the anisotropy parameterized by $v_3 = \frac{\sqrt{3}a\gamma_3}{2\hbar}$. As a result, the Fermi line in bilayer graphene may undergo a topological (Lifshitz) transition[6]: from singly connected at high carrier density, $n_{e(h)} > n_L$ to four separate pockets in momentum space, for $n_{e(h)} < n_L$. It is common for two-dimensional electron systems[7] that electron-electron (e-e) repulsion renormalizes the single-particle dispersion of carriers. In monolayer graphene, where electrons have a characteristic Dirac spectrum, this leads[8] to an increase of the Dirac velocity, from $v = \frac{\sqrt{3}a\gamma_0}{2\hbar}$ to $v(p) = v\left(1 + \frac{\alpha}{4}\ln(\Lambda/p)\right)$ with $\alpha = e^2/\epsilon_s v$. In this Communication we investigate the effect of the e-e interaction on the split-band gap γ_1, the effective mass m, and the dispersion anisotropy parameter v_3. We show for the bilayer that in the Hartree-Fock theory the e-e repulsion increases γ_1 and v_3, but renormalizes the effective mass[9] and the Lifshitz transition density downwards. Also, we find that, in contrast to the monolayer, these corrections to the electronic spectrum do not contain infrared divergencies, and that the renormalization of n_L is weak, so that the single-particle tight-binding model gives a realistic estimation[10] for the Lifshitz transition density in bilayers.

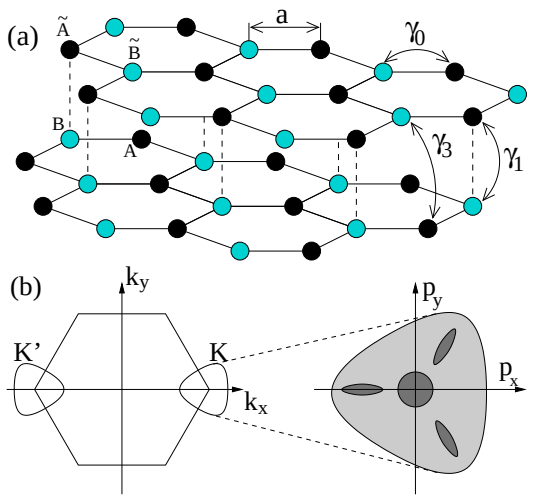

FIG. 1: (Color online) (a) The crystalline structure of bilayer graphene. (b) The first Brillouin zone and the constant energy cuts about the K, K' points. The dark shaded area represents the four pockets in momentum space filled by electrons in the gas with $|n| < n_L$ below the Lifshitz transition density, the light shaded area is the simply connected Fermi line for higher densities.

The theory presented below is based on the four-band model[3] describing electrons in bilayer graphene in the vicinity of the valley centers corresponding to the K ($\xi = 1$) and K' ($\xi = -1$) first Brillouin zone corners [see Fig. 1(b)]. The 4×4 tight-binding Hamiltonian,

$$\hat{H} = \xi \begin{pmatrix} 0 & v_3\pi & 0 & v\overline{\pi} \\ v_3\overline{\pi} & 0 & v\pi & 0 \\ 0 & v\overline{\pi} & 0 & \xi\gamma_1 \\ v\pi & 0 & \xi\gamma_1 & 0 \end{pmatrix}, \quad \begin{aligned} \pi &= p_x + ip_y, \\ \overline{\pi} &= p_x - ip_y, \end{aligned} \qquad (1)$$

which will be the subject of renormalization by the e-e interaction, is written in the basis of sublattice Bloch states $[\psi_A, \psi_{\widetilde{B}}, \psi_{\widetilde{A}}, \psi_B]$ in valley K and $[\psi_{\widetilde{B}}, \psi_A, \psi_B, \psi_{\widetilde{A}}]$ in valley K'. Notice that $\hat{H}$ has a natural ultraviolet momentum cutoff about $\Lambda \sim 1/a$. This Hamiltonian determines four bands[3], $\pm\epsilon_{1,2}(p)$. Two split-off bands $\pm\epsilon_2$ start at energies $\pm\gamma_1$. For small values of momentum, $vp \ll \gamma_1/4$, the two low-energy bands $\pm\epsilon_1$ that touch

each other at K/K' can be attributed to a 2×2 effective Hamiltonian[3]

$$\hat{H}' \approx -\frac{1}{2m}\begin{pmatrix} 0 & \overline{\pi}^2 \\ \pi^2 & 0 \end{pmatrix} + \xi v_3 \begin{pmatrix} 0 & \pi \\ \overline{\pi} & 0 \end{pmatrix}, \qquad (2)$$

where $m = \frac{\gamma_1}{2v^2}$, and $\hat{H}'$ acts on $[\psi_A, \psi_{\widetilde{B}}]$ in valley K and $[\psi_{\widetilde{B}}, \psi_A]$ in valley K'. The second term in $\hat{H}'$ causes a triangular distortion of the electronic dispersion illustrated in Fig. 1(b), where the Lifshitz transition of the electron Fermi line topology is explained, as a singly-connected line $\epsilon_1(p) = E$ splits into four disconnected pockets at $E < \epsilon_L = \frac{\gamma_1 v_3^2}{2v^2}$, which would occur at a critical density[10] ($\hbar$ restored)

$$n_L = \frac{\gamma_1^2}{2\pi\hbar^2 v^2}\left(\frac{v_3}{v}\right)^2. \qquad (3)$$

In the Hartree-Fock approximation, the change in the single-particle Hamiltonian $\widetilde{H} = \hat{H} + \hat{\Sigma}$ for electrons can be described using the self-energy diagram

$\hat{\Sigma}$ = 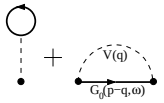 (4)

where the solid line denotes the causal Green's function of electrons in the bilayer and the dashed line stands for the interaction $\widetilde{V}(q) = 2\pi e^2/\epsilon_s q\chi(q)$, where ϵ_s is the dielectric constant of the environment ($\epsilon_s = \frac{1+4.5}{2} = 2.75$ on a SiO_2 substrate). The first (Hartree) diagram in Eq. (4), together with the positive background charge cancels the momentum-independent energy shift determined by the second (Fock) term. Below, the contribution from the Fock term is estimated both for the bare Coulomb interaction, $V(q) = 2\pi e^2/\epsilon_s q$ and for the screened Coulomb interaction, where the dielectric function $\chi(q)$ is evaluated in the random phase approximation (RPA). The self-energy $\hat{\Sigma}$ is evaluated for bilayer graphene at zero doping. Since the Lifshitz transition occurs at very low doping level, using the renormalized value of the bilayer parameters that result from this approximation is justified as long as the critical Fermi energy of this transition remains small in comparison to the energy scale γ_1.

In the 4×4 representation the self-energy is a matrix,

$$\hat{\Sigma}(\xi,\mathbf{p}) = \int \frac{d\mathbf{q}}{(2\pi)^2}\frac{\widetilde{V}(q)}{2(\widetilde{\epsilon}_1+\widetilde{\epsilon}_2)}\left[\xi v\left(1+\frac{v^2|\mathbf{q}+\mathbf{p}|^2}{\widetilde{\epsilon}_1\widetilde{\epsilon}_2}\right)\begin{pmatrix} 0 & 0 & 0 & \overline{\kappa}+\overline{\pi} \\ 0 & 0 & \kappa+\pi & 0 \\ 0 & \overline{\kappa}+\overline{\pi} & 0 & 0 \\ \kappa+\pi & 0 & 0 & 0 \end{pmatrix} + \gamma_1\left(1+\frac{v_3^2|\mathbf{q}+\mathbf{p}|^2}{\widetilde{\epsilon}_1\widetilde{\epsilon}_2}\right)\begin{pmatrix} 0&0&0&0\\0&0&0&0\\0&0&0&1\\0&0&1&0\end{pmatrix}\right.$$
$$\left. - \frac{\gamma_1}{|\mathbf{q}+\mathbf{p}|^2}\begin{pmatrix} 0 & (\overline{\kappa}+\overline{\pi})^2 & 0 & 0 \\ (\kappa+\pi)^2 & 0 & 0 & 0 \\ 0 & 0 & 0 & 0 \\ 0 & 0 & 0 & 0 \end{pmatrix} + \xi v_3\left(1-\frac{\gamma_1^2}{\widetilde{\epsilon}_1\widetilde{\epsilon}_2}\right)\begin{pmatrix} 0 & \overline{\kappa}+\overline{\pi} & 0 & 0 \\ \kappa+\pi & 0 & 0 & 0 \\ 0 & 0 & 0 & 0 \\ 0 & 0 & 0 & 0 \end{pmatrix} + \dots\right]. \qquad (5)$$

Here, we omitted two unimportant terms, and define $\kappa = q_x + iq_y$, $\pi = p_x + ip_y = pe^{i\phi}$, and $\widetilde{\epsilon}_{1,2} \equiv \epsilon_{1,2}(\mathbf{q}+\mathbf{p})$ with

$$\epsilon_\alpha^2(\xi,\mathbf{p}) = \frac{\gamma_1^2}{2} + \left(v^2+\frac{v_3^2}{2}\right)p^2 + (-1)^\alpha\sqrt{\frac{1}{4}\left(\gamma_1^2 - v_3^2p^2\right)^2 + v^2p^2\left(\gamma_1^2+v_3^2p^2\right) + 2\xi\gamma_1 v_3 v^2 p^3\cos 3\phi}. \qquad (6)$$

The self-energy $\hat{\Sigma}$ in Eq. (5) is ω-independent, as usual in the Hartree-Fock approximation. Schematically, the result of integration over $\mathbf{q}$ in Eq. (5) can be represented as

$$\hat{\Sigma}(\xi,\mathbf{p}) = e^2\begin{pmatrix} 0 & \overline{B}+Z & 0 & \overline{A} \\ B+\overline{Z} & 0 & A & 0 \\ 0 & \overline{A} & 0 & C \\ A & 0 & C & 0 \end{pmatrix}, \qquad (7)$$

where $A = \xi A_1\pi + O(p^2)$, $C = \frac{\gamma_1}{v}C_0 + O(p^2)$, $B = \frac{\xi v_3}{v}B_1\overline{\pi} + \frac{v}{\gamma_1}B_2\pi^2 + O(p^3)$, and $Z = \frac{\xi v_3}{v}M_1\pi + O(p^3)$. Here we expanded $\hat{\Sigma}$ in powers of p, in order to keep only the terms relevant for the renormalization of the bilayer parameters v, v_3, γ_1, m and n_L. Term A in Eq. (7) takes into account the correction to the intra-layer velocity v. A similar effect is known to occur in monolayers[8]. Term C in Eq. (7) modifies the inter-layer coupling γ_1. The part of terms B and Z that is linear in $\pi, \overline{\pi}$ yields renormalization of v_3. The quadratic part of term B combines with A and C to determine the renormalization of the effective mass,

$$\widetilde{m}^{-1} = \frac{2v^2}{\gamma_1}\left[1+\alpha\left(2A_1 - C_0 + \frac{1}{2}B_2\right)\right], \quad \alpha = e^2/v\epsilon_s,$$

which is a result similar to that obtained by Borghi *et al*[9]. Together, all of these determine the shift of the Lifshitz

	bare Coulomb (any ϵ_s)	screened suspended ($\epsilon_s = 1$)	screened on SiO_2 ($\epsilon_s = 2.75$)
A_1	$(0.58 \div 0.66) + \frac{1}{4}\ln(v\Lambda/\gamma_1)$	$(0.03 \div 0.04) + 0.032\ln(v\Lambda/\gamma_1)$	$(0.076 \div 0.098) + 0.071\ln(v\Lambda/\gamma_1)$
B_1	-0.063	-0.0013	-0.0034
B_2	0.38	0.016	0.039
C_0	$(0 \div 0.36) + \frac{1}{4}\ln(v\Lambda/\gamma_1)$	$(-0.025 \div -0.14) + 0.032\ln(v\Lambda/\gamma_1)$	$(-0.047 \div -0.021) + 0.071\ln(v\Lambda/\gamma_1)$
M_1	$(0.7 \div 1.1) + \frac{1}{8}\ln(v\Lambda/\gamma_1)$	$(0.036 \div 0.082) + 0.032\ln(v\Lambda/\gamma_1)$	$(0.09 \div 0.19) + 0.071\ln(v\Lambda/\gamma_1)$

TABLE I: The physical parameters of the self-energy $\hat{\Sigma}(\xi, \mathbf{p})$ (Eq. (7)), for the bare and screened Coulomb interaction. Where two limits are given, they correspond to integrating the finite (not logarithmically divergent) part up to $q = \frac{\gamma_1}{v}$ and to $q = \infty$, respectively.

transition density,

$$\widetilde{n}_L = n_L\left(1 + 2\alpha\left(C_0 + M_1 + B_1 - 2A_1\right)\right). \qquad (8)$$

The numerical values of the coefficients A_1, B_1, B_2, C_0, and M_1 in Eq. (7) were calculated for suspended graphene flakes and flakes on SiO_2 substrate with and without screening of the Coulomb interaction taken into account[11] (Table I).

Screening of the e-e interaction in graphene is taken into account in the RPA, by the effective static dielectric function

$$\chi(\mathbf{q}) = 1 - V(\mathbf{q})\Pi(\mathbf{q}),$$
$$\Pi(\mathbf{q}) = -i\int \frac{d\omega d\mathbf{p}}{(2\pi)^3}\mathrm{Tr}\left(\hat{G}_0(\mathbf{p}+\frac{\mathbf{q}}{2},\omega)\hat{G}_0(\mathbf{p}-\frac{\mathbf{q}}{2},\omega)\right),$$

where $\Pi(\mathbf{q})$ is the polarizability of the electron gas. Fig. 2 shows the numerical evaluation of $\Pi(q)$, which deviates from the constant value[12] $\approx -0.44\gamma_1/v^2$ obtained earlier using the two-band Hamiltonian $\hat{H}'$ at $q \sim \gamma_1/2v$, where the band has a crossover from parabolic to an almost linear behavior. To obtain analytical asymptotic expressions in the relevant limits first, consider $q > q_* \gtrsim \gamma_1/v$, where the dominant contribution comes from $p \gg \gamma_1/v$, and the free electron Green's function reduces to the free Green's function of two decoupled monolayers. Then[8], $\Pi = -\frac{1}{16}Nq/v$ with $N = 8$, and

$$\widetilde{V}(q > q_*) = \frac{2\pi e^2}{(1+\alpha\pi)q}. \qquad (9)$$

For $q < q_*$, where the electron dispersion is mostly parabolic, screening has the form of Thomas-Fermi screening with the radius $r_0 = 0.17v/\gamma_1$ (for $\epsilon_s = 1$). A sufficient simultaneous analytical description of both regimes can be done using an interpolation formula,

$$\widetilde{V}(q < q_*) = (\beta + \theta q^2 + \eta q^4)e^{-wq^2}, \qquad (10)$$

where the parameters β, γ, η, w are determined by a numerical fit shown in Fig. 2, and the value of q_* is determined from the intersection of $\widetilde{V}(q < q_*)$ and $\widetilde{V}(q > q_*)$.

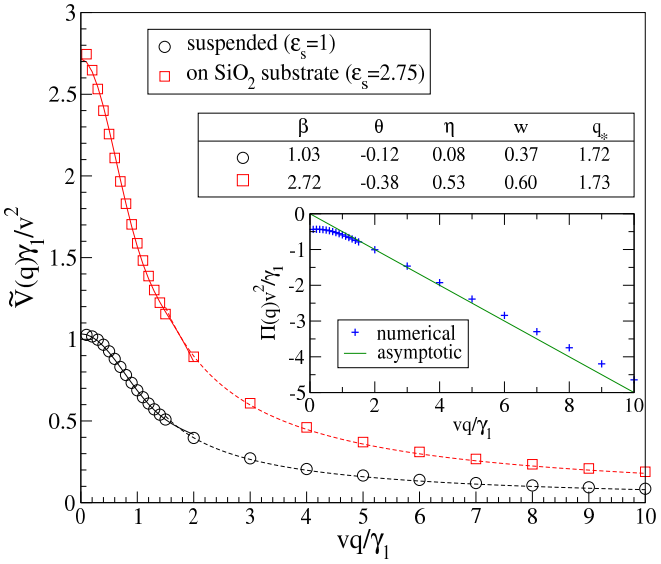

FIG. 2: (Color online) The renormalized interaction[11] $\widetilde{V}(q)$ from numerics (symbols), its large momentum asymptotics Eq. (9) (dashed line) and low-momentum asymptotics Eq. (10) (solid line) for $\epsilon_s = 1$ and 2.75. Inset: the static polarization $\Pi(q)$ from numerics and its asymptotics. Table: parameters of the small q approximate interaction (Eq. (10)).

Finally, we determine that the bilayer parameters are renormalized by the e-e repulsion as

$$\frac{\widetilde{v}}{v} = 1 + \frac{\widetilde{\alpha}Y}{4} + \delta_v, \quad \frac{\widetilde{v}_3}{v_3} = 1 + \frac{\widetilde{\alpha}Y}{8} + \delta_{v_3}, \qquad (11)$$
$$\frac{\widetilde{\gamma}_1}{\gamma_1} = 1 + \frac{\widetilde{\alpha}Y}{4} + \delta_{\gamma_1}, \quad \frac{\widetilde{m}^{-1}}{m^{-1}} = 1 + \frac{\widetilde{\alpha}Y}{4} + \delta_{m^{-1}},$$
$$Y = \ln(v\Lambda/\gamma_1),$$

where the numerical values of all δ's are listed in Table II. This result shows that the intralayer velocity v, the interlayer hopping γ_1, and the trigonal distortion parameter v_3 are all enhanced by the e-e interaction[11]. With bare Coulomb interaction this enhancement would be grossly overestimated if we used the actual value $\alpha = e^2/\hbar v \approx 2.19$ for graphene.

However, after screening is taken into account, we find

	$\widetilde{\alpha}$	δ_v	δ_{v_3}	δ_{γ_1}	$\delta_{m^{-1}}$
I	$\frac{e^2}{\hbar v \epsilon_s}$	$0.58 \div 0.66$	$0.67 \div 1.05$	$0 \div 0.36$	$1.00 \div 1.51$
II	0.28	$0.07 \div 0.09$	$0.08 \div 0.18$	± 0.05	$0.17 \div 0.20$
III	0.20	$0.06 \div 0.08$	$0.07 \div 0.15$	± 0.04	$0.17 \div 0.19$

TABLE II: Constants for Eq. (11) for bare Coulomb interaction (I), screened Coulomb interaction in suspended graphene (II), and screened Coulomb interaction in graphene on SiO_2 substrate (III).[11] Where two limits are given, they correspond to integrating the finite (not logarithmically divergent) part up to $q = \gamma_1/v$ and to $q = \infty$, respectively.

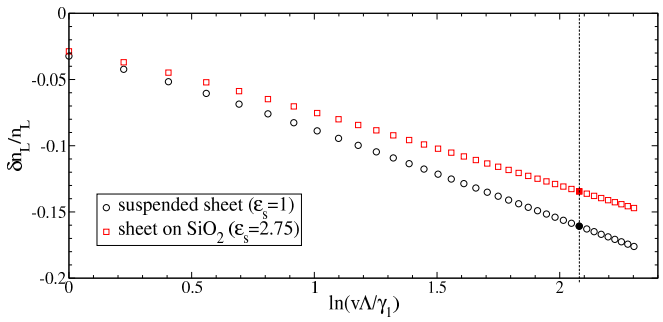

FIG. 3: (Color online) The relative reduction $\delta n_L/n_L = \widetilde{n}_L/n_L - 1$ of the Lifshitz transition density by the e-e interaction for a suspended sheet and one on SiO_2 substrate. The vertical line shows the estimation for $\Lambda \approx \gamma_0/v$.

that one has to usein Eq. (11) $\widetilde{\alpha} \approx 0.28$ for a suspended flake and $\widetilde{\alpha} \approx 0.20$ for a flake on SiO_2, which gives a much weaker renormalization effect than an estimate using bare Coulomb interaction. Also, using Eqs. (8) and (11), one may see that in the theory ignoring screening the renormalization of the Lifshitz transition density n_L would be hugely overestimated, resulting in its disappearance ($n_L \to 0$). However, having taken into account the effect of the reduction of the e-e repulsion by screening, we find a much smaller shift in the value of n_L from that determined using the tight-binding model for noninteracting electrons[3,10]. The calculated shift in the transition density n_L for the screened Coulomb interaction is shown in Fig. 3 as a function of momentum cutoff Λ, with the vertical line corresponding to $\Lambda \approx \gamma_0/v$. This determines an approximately 15% reduction of the Lifshitz transition density for a suspended sheet and about 12% for a bilayer on a SiO_2 substrate.

The result of the above-presented analysis of the bilayer band parameters and the Lifshitz transition density n_L suggests that their renormalization by the e-e repulsion is relatively weak, due to the screening of the e-e interaction by the electrons themselves. Thus, we conclude that the Lifshitz transition is not trivially hindered by many-body effects. The Lifshitz transition can be detected through the singularity of the thermopower[6] that develops when a neck forms from the central pocket to the side pockets of the Fermi line in bilayer graphene (Fig. 1(b)). Such an observation would require samples of high homogeneity, but in contrast to bulk metals for which the Lifshitz transition was first discussed, such an experiment would be possible in graphene since the carrier density in graphene can be directly controlled using external gates.

We thank O. Kashuba for useful discussions and help throughout this work. This work was supported by the Lancaster University-EPSRC Portfolio Partnership.

[1] K. S. Novoselov, E. McCann, S. V. Morozov, V. I. Falko, M. I. Katsnelson, U. Zeitler, D. Jiang, F. Schedin, and A. K. Geim, Nat. Phys. **2**, 177 (2006).

[2] J. D. Bernal, Proc. Roy. Soc. A **106**, 749 (1924).

[3] E. McCann and V. I. Fal'ko, Phys. Rev. Lett. **96**, 086805 (2006); S. Latil, L. Henrard, Phys. Rev. Lett. **97**, 036803 (2006); B. Partoens, F. M. Peeters, Phys. Rev. B **74**, 075404 (2006); M. Koshino, T. Ando, Phys. Rev. B **73**, 245403 (2006); F. Guinea, A.H. Castro Neto, N. M. R. Peres, Phys. Rev. B **73**, 245426 (2006); J. Nilsson, A. H. Castro Neto, N. M. R. Peres, and F. Guinea, Phys. Rev. B **73**, 214418 (2006); G. P. Mikitik and Y. V. Sharlai, Phys. Rev. B **77**, 113407 (2008).

[4] T. Ohta, A. Bostwick, Th. Seyller, K. Horn, and E. Rotenberg, Science **313**, 951 (2006);

[5] A. B. Kuzmenko, E. van Heumen, D. van der Marel, P. Lerch, P. Blake, K. S. Novoselov, and A. K. Geim, arXiv:0810.2400 (2008); L. M. Malard, J. Nilsson, D. C. Elias, J. C. Brant, F. Plentz, E. S. Alves, A. H. Castro Neto, and M. A. Pimenta, Phys. Rev. B **76** 201401(R) (2007); A. Das, B. Chakraborty, S. Piscanec, S. Pisana, A. K. Sood, and A. C. Ferrari, arXiv:0807.1631 (2008); L. M. Zhang, Z. Q. Li, D. N. Basov, M. M. Fogler, Z. Hao and M. C. Martin, Phys. Rev. B **78**, 235408 (2008); Z. Q. Li, E. A. Henriksen, Z. Jiang, Z. Hao, M. C. Martin, P. Kim, H. L. Stormer, and D. N. Basov, Phys. Rev. Lett. **102**, 037403 (2009).

[6] L. M. Lishitz, Zh. Exp. Teor. Fiz., **38**, 1565 (1960), i.e. Sov. Phys. JETP **11**, 1130 (1960); A. A. Abrikosov, *Fundamentals of the Theory of Metals.* Elsevier, 1988.

[7] G. F. Giuliani and G. Vignale, *Quantum Theory of the Electron Liquid.* Cambridge University Press, 2005.

[8] J. González, F. Guinea, and M. A. H. Vozmediano, Phys. Rev. B **59**, R2474 (1999); T. Ando, J. Phys. Soc. Jpn. **75**, 074716 (2006); O. Vafek, Phys. Rev. Lett. **98**, 216401 (2007); B. Wunsch, T. Stauber, F. Sols, and F. Guinea, New J. Phys. **8**, 318 (2006); E. H. Hwang and S. Das Sarma, Phys. Rev. B **75**, 205418 (2007).

[9] G. Borghi, M. Polini, R. Asgari, and A. H. MacDonald, arXiv:0902.1230 (2009).

[10] Using bulk graphite parameters, $\gamma_0 = 3.1$ eV, $\gamma_1 = 0.39$ eV, and $\gamma_3 = 0.315$ eV, $n_L = 6 \times 10^{10}\text{cm}^{-2}$; c.f. M. S. Dresselhaus and G. Dresselhaus, Adv. Phys. **51**, 1 (2002); R. C. Tatar and S. Rabii, Phys. Rev. B **25**, 4126 (1982);

J.-C. Charlier, X. Gonze, and J.-P. Michenaud, Phys. Rev. B **43**, 4579 (1991).

[11] Recall that the renormalization by the e-e interaction was calculated for zero doping. We anticipate these values to be applicable at low doping.

[12] E. H. Hwang and S. Das Sarma, Phys. Rev. Lett. **101**, 156802 (2008).